Experimental investigation of a thermally integrated Carnot battery using a reversible heat pump/organic Rankine cycle

Olivier DUMONT[1]*, Antonios CHARALAMPIDIS[2], Vincent LEMORT[1] and Sotirios KARELLAS[2]

[1]Thermodynamics Laboratory, University of Liège
Liège, Belgium
olivier.dumont@uliege.be, vincent.lemort@uliege.be

[2]Laboratory of Steam Boilers and Thermal Plants, National Technical University of Athens,
Athens, Greece
antonishar@mail.ntua.gr, sotokar@mail.ntua.gr

* Corresponding Author

ABSTRACT

The growth of renewable energy requires flexible, low-cost and efficient electrical storage systems to balance the mismatch between energy supply and demand. The Carnot battery (or Pumped Thermal Energy Storage) converts electric energy to thermal energy with a heat pump (HP) when electricity production is greater than demand; when electricity demand outstrips production, the Carnot battery generates power from two thermal storage reservoirs (Rankine mode). Classical Carnot batteries architectures do not achieve more than 60% roundtrip electric efficiency. However, innovative architectures, using waste heat recovery (thermally integrated Carnot batteries) are able to reach electrical power production of the power cycle larger than the electrical power consumption of the heat pump (power-to-power-ratio), increasing the value of the technology. It can be shown that the optimization of such a technology is a trade-off between the maximization of the power and the power-to-power ratio (depending on electricity prices among others). In this paper, the full development of a prototype of thermally integrated Carnot battery using a reversible heat pump/organic Rankine cycle (HP/ORC) is described. It includes the selection of the nominal design point, the architecture, the components and the sizing. This first experimental campaign showed a roundtrip electrical energy ratio of 72.5% with ORC efficiency of 5% (temperature lift is equal to 49 K) and COP of HP of 14.4 (temperature lift is equal to 8 K). These results are very encouraging because the performance can easily be improved (probably up to 100% roundtrip electrical energy ratio) by optimizing the volumetric machine, working at larger scale, optimizing the control and thermal insulation. Also, the performance of the main components (volumetric machine and heat exchangers) is analyzed.

1. INTRODUCTION

1.1 Context

The share of electricity production needs to increase sharply in the next decades to decrease the impact of humans on the environment. However, there is a significant mismatch between renewable energy production and consumption. This means that electrical energy storages will play a very important role in the future. Among the available technologies, Gravity Energy Storage, Compressed Air Energy Storage and Pumped Hydro Storage are site dependent, Fuel Cells can only achieve low efficiency up to now and electrical batteries suffer from high costs and the use of rare materials (Benato et al., 2018). A recent alternative technology has been therefore studied for several years: the Carnot battery (or Pumped Thermal Energy Storage).

The principle is rather simple: a heating cycle converts electricity into thermal energy, to store it and to use a power cycle to convert it back to electrical energy when needed. Different configurations are possible to achieve a Carnot

battery: a closed Brayton cycle (Smallbone, 2019; Malta, 2019), an electrical heater combined with a Rankine Cycle (Siemens, 2019), a heat pump (HP) combined with a Rankine cycle (CHESTER, 2019; Dumont et al., 2020), the Lamm-Honigmann process (Janhke et al., 2013) or Liquid Air Energy Storage (Laughhead, 2018). The performance of the system can be improved by integrating waste heat into the process (Steinman et al., 2014; Dumont et al., 2019). The configuration using a heat pump and a Rankine cycle is particularly suited for this thermal integration because of its low range of temperature. Recently, it was proposed to decrease the costs of this system by having only one system acting as a heat pump or as an organic Rankine cycle (ORC) with the same components: the reversible HP/ORC system (Dumont et al., 2015; Dumont, 2017).

1.2 Concept

The concept of Carnot battery with a reversible HP/ORC power system configuration using waste heat is presented in Figure 1. When there is an excess of electricity on the grid, the charging mode can be activated through the heat pump. It increases the waste heat temperature up to the thermal storage temperature through a classical cycle (evaporator, compressor, condenser and expansion valve). The use of waste heat allows the heat pump to work with a high Coefficient of Performance (COP). On the contrary, when the electrical consumption is high on the electrical grid, the system is reversed and is able to work as an ORC power system. The heat from the thermal energy storage is converted into electricity through a classical cycle composed of a pump, an evaporator, an expander and an air-cooled condenser.

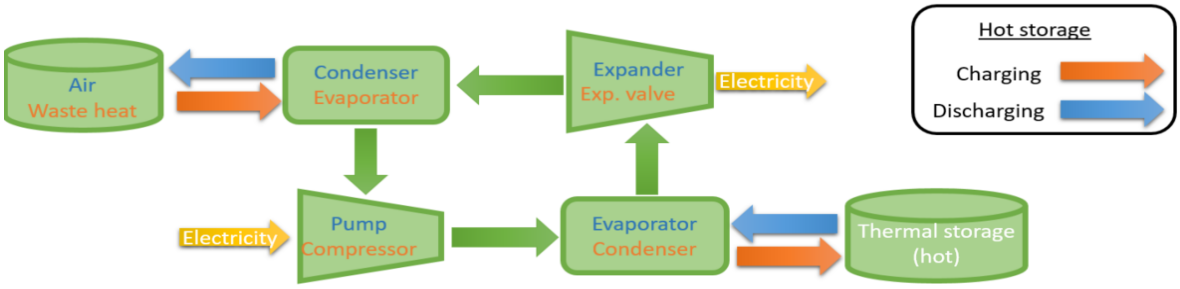

Figure 1: Concept of Carnot battery with a reversible HP/ORC power system using waste heat (Dumont et al., 2020)

After a brief context and description of the concept of the Carnot battery using a reversible HP/ORC power system (Section 1 – Introduction), this paper describes the test-rig with the technical specifications of the sensors and of the components (Section 2 – Methodology). Following this, the results section (Section 3) provides the performance indicators of each component and of the global cycle. From that point, a discussion about the results leads to a better understanding of these machines. Finally, the last section concludes and sets opportunities for further research.

2. METHODOLOGY – EXPERIMENTAL SETUP

2.1 Layout

The sizing and the nominal conditions of the system is extensively described in Dumont et al. (2020). Figure 2 shows a hydraulic scheme with all the components and sensors. The dark blue loop is the refrigerant loop composed of a high-pressure (hp) heat exchanger, a scroll volumetric machine able to work as a compressor or as an expander, a low-pressure (lp) heat exchanger, and two parallel branches with an expansion valve for the heat pump and a pump for the ORC power system. The refrigerant is going clockwise for the ORC mode and counter-clockwise for the heat pump mode. The red loop (water) corresponds to the thermal energy storage loop with two storages in order to operate with a perfect stratification between the hot zone and cold zone. A circulator provides the necessary flow using a four-way valve to provide a counter flow in the hp heat exchanger. The light blue loop (water) is able to regulate both the flow and the temperature entering in the lp heat exchanger with a four-way valve for the same reason as mentioned before. This water flow simulates the waste heat in HP mode and the air-cooled condenser in ORC mode.

2.2 Components

The components specifications are described in Table 1. The volumetric machine is a scroll compressor from the automotive industry, which has been modified to be able to work as an expander. The ORC pump is a plunger pump because of its high volumetric and isentropic efficiency (Dumont et al., 2015). Regarding the expansion valve, no electronic expansion valve exists for the selected refrigerant (R1233zd(E)). A solenoid valve is therefore used to adjust

the compressor suction superheating in heat pump mode. Two 900 liters storages are used to store 10 kWh of energy. The condenser and the evaporator are plate heat exchangers, sized to keep the pinch point below 2 K.

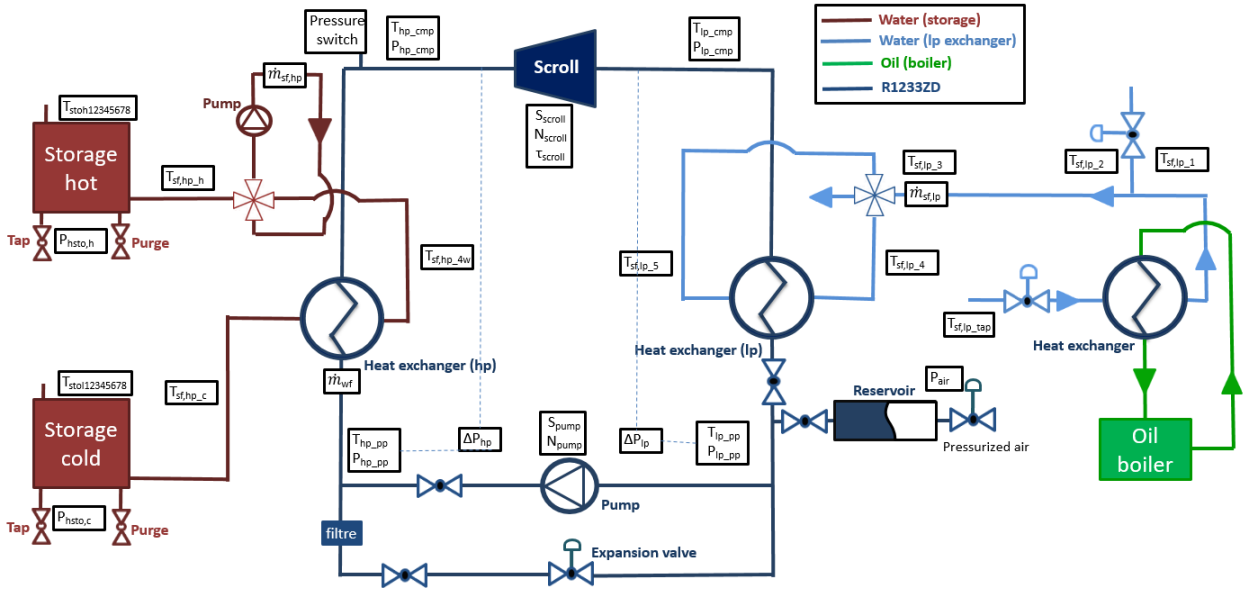

Figure 2: Hydraulic scheme of the Carnot battery test-rig

Table 1: Technical data of the components

Component	Parameter	Value
Compressor Sanden TRSA09	Swept volume [cm^3]	85.7
	Shaft speed [RPM]	[500-8000]
	Volume ratio	2.2
	Power [W]	1300
Plunger pump Hyproplunger 2220B-P	Flow rate [l/s]	0.159
	Shaft speed [RPM]	1725
	Maximum pressure [bar]	137
Expansion valve Asco 290	Flow coefficient – K_v [m^3/h]	2.7
	Maximum temperature [°C]	90
	Maximum differential pressure [bar]	6
Auxiliary pump (hp) Grundfos CRE1-4	Maximum flow [l/s]	0.5
	Head [m]	15
	Maximum temperature [°C]	95
Liquid tank	Maximum pressure [bar]	10
	Volume [l]	5
	Maximum temperature [°C]	110
Storage (x2)	Volume [m^3]	0.9 (x2)
lp heat exchanger B85Hx44	Area [m^2]	2.52
	Number of plates [-]	44
hp heat exchanger B26Hx060	Area [m^2]	2.38
	Number of plates [-]	60

2.3 Sensors

The test-rig is fully equipped with high accuracy sensors (Table 2).

Table 2: Technical data of the sensors

Sensor	Parameter	Value
Pressure Keller PAA23/0-10bar	Range [bar]	[0-10]
	Maximum pressure [bar]	20
	Accuracy [bar]	0.005
Wattmetre Gossen A2000	Range [W]	[-2000:2000]
	Accuracy [W]	10
Torquemetre ETH DRVL-II	Range [Nm]	20
	Accuracy [Nm]	0.02
Secondary fluid mass flowrate ROSEMOUNT 8732E	Range [l/s]	[0-1]
	Accuracy [% FS]	0.5
Working fluid mass flow rate Micro motion F025S	Range [kg/s]	[0.005-0.135]
	Accuracy [% FS]	0.2

2.4 Performance criteria

The most used criterion to characterize the performance of a heat pump (ORC, resp.) is the Coefficient of Performance (COP) according to Equation (1) (the efficiency of the ORC, resp., according to Equation 2).

$$COP = \frac{\dot{Q}_{cd,r,oil}}{\dot{W}_{cp,el}} \tag{1}$$

$$\eta_{global} = \frac{\dot{W}_{exp,el} - \dot{W}_{pp,el}}{\dot{Q}_{ev,r,oil}} \tag{2}$$

The characterization of the compressor is performed with the isentropic efficiency (Equation 3) and the volumetric efficiency (Equation 4).

$$\varepsilon_{cp,is} = \frac{\dot{m}_r(h_{r,cp,ex,is} - h_{r,cp,su}) + \dot{V}_{oil}(p_{cp,ex} - p_{cp,su})}{\dot{W}_{cp,el}} \tag{3}$$

$$\varepsilon_{cp,vol} = \frac{\dot{V}_{cp,su,tot}}{\dot{V}_{cp,th}} \tag{4}$$

For the expander, Equation (5) is used for the isentropic efficiency and Equation (6) for the filling factor (i.e. the volumetric efficiency of the expander).

$$\varepsilon_{exp,is} = \frac{\dot{W}_{exp,el}}{\dot{m}_r(h_{r,exp,su} - h_{r,exp,ex,is}) + \dot{V}_{oil}(p_{exp,su} - p_{exp,ex})} \tag{5}$$

$$FF_{exp} = \frac{\dot{V}_{exp,su,tot}}{\dot{V}_{exp,th}} \tag{6}$$

3. RESULTS AND DISCUSSION

3.1 Range of operating conditions

Concerning the experimental campaign, 62 (60, resp.) steady-state points have been performed in ORC mode (HP mode, resp.). The measurements are given in Appendices (Table 5 and Table 6). The test-rig has been exploited in a wide range of operating conditions (Table 3).

Table 3: Operating conditions

Parameter	ORC	HP
Evaporator thermal power [W]	[8423-18183]	[1203-13351]
Condenser thermal power [W]	[725-16231]	[1326-14495]
Evaporation pressure [bar]	[3.4-5.8]	[0.65-4.9]
Condensation pressure [bar]	[1.1-1.9]	[1.6-7.2]
Mass flow rate [kg/s]	[0.034-0.079]	[0.007-0.084]
Subcooling [K]	[6.2-8.8]	[4.1-28.9]
Superheating [K]	[4.0-25.7]	[3.3-6.3]

3.2 Measurements validation

Experimental campaigns are often subject to measurements issues such as sensors malfunction, operator misuse or data acquisition failure. Therefore, it is of primary importance to crosscheck the experimental data for consistency using all possible redundancies in the measured data, performing heat balances on all components and checking that the measured data is self-consistent. The following verifications have been performed:

- Global residual (Equation (7), Appendices Figures 6-7):

$$Res_{global} = \dot{Q}_{ev,w} + \dot{W}_{cp/exp,el} - \dot{Q}_{cd,w} + (\dot{W}_{pp,el}) \quad (7)$$

- Heat balance on the condenser and evaporator (Equation (8), Appendices Figures 8-9):

$$\dot{m}_r(h_{r,su} - h_{r,ex}) + \dot{m}_{oil}(h_{oil,su} - h_{oil,ex}) = \dot{m}_w . cp_w(t_{w,ex} - t_{w,su}) \quad (8)$$

- Residual on the compressor and expander (Equation (9), Appendices Figures 10-11):

$$Res_{cp} = \dot{W}_{cp,el} - \dot{m}_r(h_{r,ex} - h_{r,su}) - \dot{m}_{oil}(h_{oil,ex} - h_{oil,su}) - \dot{V}_{oil}(p_{ex} - h_{su}) - \dot{Q}_{cp,amb} \quad (9)$$

The verifications show that the residual of each balance is lower than the uncertainty propagation error for the different components for almost all the points. The few exceptions encountered can be explained by the solubility of oil and ambient losses not having been taken into account.

3.3 Global performance

In this paper, the temperature lift is the absolute value of the difference between the condensation and evaporation pressure. The global performance of the system is presented in terms of net electrical production of the ORC, ORC efficiency and COP of the HP in Figure 3. As expected (Dumont et al., 2019), the COP reaches high values for low lifts. On the contrary, the performance of the ORC is improved in terms of power production and efficiency by increasing the lift. Those numbers are slightly lower than the nominal sizing conditions because the expander presents a rather low isentropic efficiency (see Section 3.4). However, the roundtrip electrical energy ratio (product of the ORC efficiency and the COP) is equal to 72.5%, which is rather high due to the small size of the system and the use of only one volumetric machine for both modes.

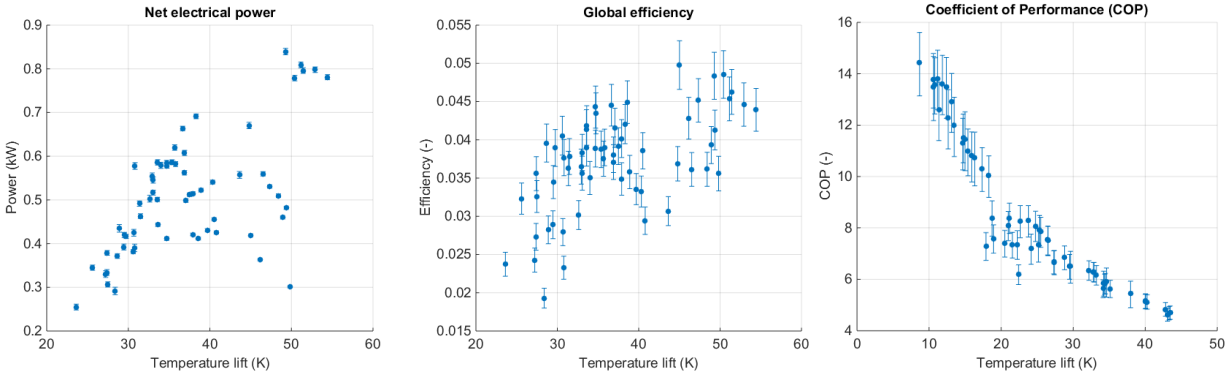

Figure 3: Global performance of the reversible HP/ORC system (ORC net power and efficiency and COP)

3.4 Volumetric machine

The performance of the scroll machine is presented in terms of mechanical power, isentropic and volumetric efficiency against its shaft speed (Figures 4-5). The expander filling factor is decreasing with the shaft speeds due to the smaller influence of the internal leakages at higher mass flow rates. The scroll efficiency only reaches 64% (compared with the value obtained in (Dumont et al., 2015)). The main explanations could be the pressure drops inside the machine due to the low cross-section area and the high pressure ratios (compared to the scroll built-in volume ratio) at points with high temperature lift. Further investigation needs to be performed to confirm this. On the other side, the compressor is rather efficient (75%) and presents a rather constant volumetric efficiency ranging between 80% and 115%.

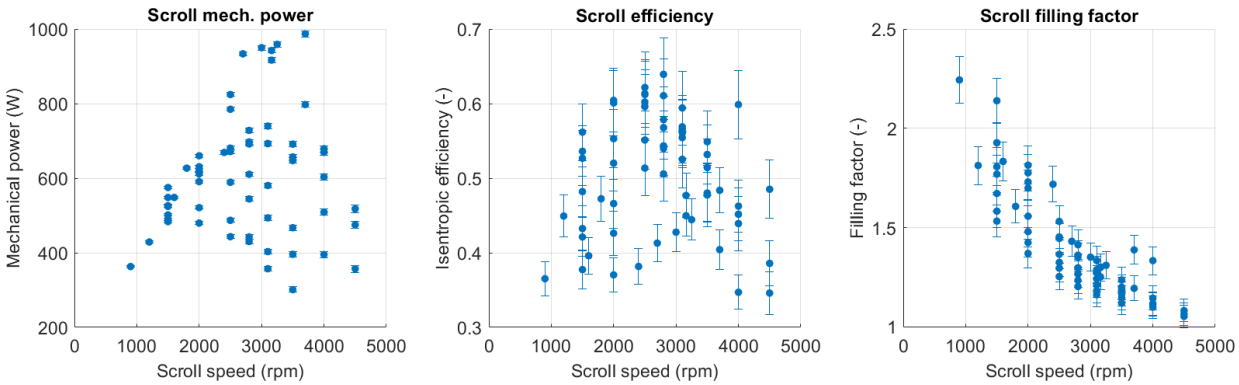

Figure 4: Expander performance in ORC mode.

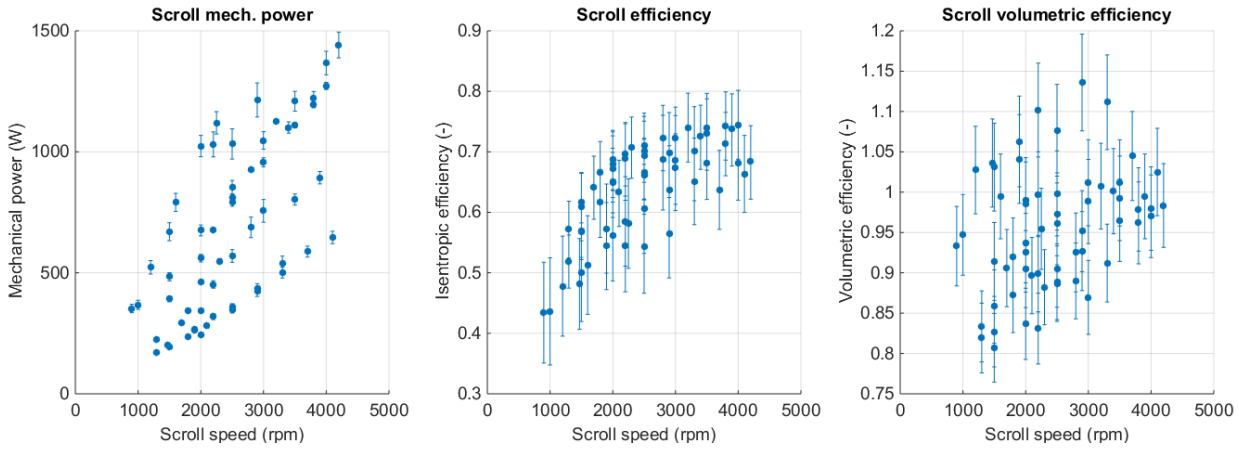

Figure 5: Compressor performance in HP mode

3.5 Heat exchangers

Heat exchangers are tricky to size (Dumont et al., 2020) because of their necessary reversibility and high performance (low pinch points and pressure drops). As shown in Table 4, all the performance indicators in ORC and HP mode show the decent sizing of the heat exchangers.

Table 4: Maximum pinch points and pressure drops of the condenser and of the evaporator

Parameter (maximum)	ORC	HP
Evaporator pressure drop [bar]	0.22	0.095
Condenser pressure drop [bar]	0.21	0.38
Evaporator pinch point [K]	6.9	3.6
Condenser pinch point [K]	0.5	0.3

4. CONCLUSIONS

This paper discusses about an innovative technology to store electricity at low cost based on a Carnot battery using a reversible HP/ORC system. A proof of concept is sized, built and tested successfully. This proves the technical feasibility of this technology by showing decent performance of components (heat exchangers and volumetric machine) that work in very different conditions depending of the operating mode. This first experimental campaign showed a roundtrip electrical energy ratio of 72.5% with ORC efficiency of 5% (lift is equal to 49 K) and COP of HP of 14.4 (lift is equal to 8 K). These results are very encouraging because the performance can easily be improved (probably up to 100% roundtrip electrical energy ratio) by optimizing the volumetric machine, working at larger scale, optimizing the control and thermal insulation. Further tests and results analysis are to be done in order to characterize this system in depth.

NOMENCLATURE

c_p	specific heat	(J/(kg-K))
ε,η	efficiency	(–)
FF	filling factor	(–)
h	specific enthalpy	(J/kg)
$\dot{m}$	mass flow rate	(kg/s)
$\dot{Q}$	thermal power	(W)
Res	residual	(W)
t	temperature	(K)
$\dot{V}$	volume flow rate	(m^3/s)
$\dot{W}$	power	(W)

Acronym

COP	Coefficient of Performance
HP	Heat Pump
ORC	Organic Rankine Cycle

Subscript

amb	ambient
cd	condenser
cp	compressor
el	electrical
ev	evaporator
ex	exhaust
exp	expander
is	isentropic
oil	oil
pp	pump
r	refrigerant
su	supply
th	theoretical
tot	total
vol	volumetric
w	water

REFERENCES

Benato A, Stoppato A. Pumped Thermal Electricity Storage: A technology overview. Therm Sci Eng Prog 2018a;6:301–15. https://doi.org/10.1016/j.tsep.2018.01.017.

Dumont, O., Quoilin, S., Lemort, V., 2015. Experimental investigation of a reversible heat pump/organic Rankine cycle unit designed to be coupled with a passive house to get a Net Zero Energy Building, International Journal of Refrigeration, 54, 190-203, https://doi.org/10.1016/j.ijrefrig.2015.03.008.

Dumont, O., 2017. Investigation of a heat pump reversible into an organic Rankine cycle and its application in the building sector, PhD Dissertation.
Dumont, O., Dickes, R., Ishmael, M., Lemort, V., 2019. Mapping of performance of pumped thermal energy storage (Carnot battery) using waste heat recovery, proceedings of the ORC 2019 conference.
Dumont, O., Reyes, A., A., Lemort, V., 2020. Modelling of a thermally integrated Carnot battery using a reversible heat pump/organic Rankine cycle, Proceedings of the ECOS conference in Japan 2020.
Jahnke, A., Strenge, L., Fleßner, V., Wolf, N., Jungnickel, T., Ziegler, F., 2013. First cycle simulations of the Honigmann process with LiBr/H2O and NaOH/H2O as working fluid pairs as a thermochemical energy storage, International Journal of Low-Carbon Technologies 2013, 8, i55–i61
Laughhead, 2018. Highview Power launches world's first grid-scale liquid air energy storage plant, https://www.highviewpower.com/wp-content/uploads/2018/07/Highview-Power-Pilsworth-Launch-Press-Release.pdf consumted on the 24/10/2019.
Malta, 2019. https://x.company/projects/malta/ consulted on the 14/10/2019.
Siemens, 2019. https://www.siemensgamesa.com/products-and-services/hybrid-and-storage/thermal-energy-storage-with-etes consulted on the 15/09/2017. Consulted on the 09/09/2019.
Smallbone, A., Jülch, V., Wardle, R., Roskilly, A., 2019. Levelised Cost of Storage for Pumped Heat Energy Storage in comparison with other energy storage technologies, Energy Conversion and Management, Volume 152, 15 November 2017, Pages 221-228.
Steinmann, W.D., 2014. The CHEST (Compressed Heat Energy STorage) concept for facility scale thermo mechanical energy storage, Energy 69, 543-552.

ACKNOWLEDGEMENT

The work documented in this publication has been funded by the 2019 Scholarship of the Knowledge Center on Organic Rankine Cycle technology (www.kcorc.org). The results were obtained by the collaboration of the Thermodynamics Laboratory of the University of Liège, Belgium and the Laboratory of Steam Boilers and Thermal Plants of the National Technical University of Athens, Greece.

APPENDICES

Table 5: Measurement data (ORC)

Test	$\dot{m}_{wf}$ (g/s)	$\dot{m}_{evap}$ (kg/s)	$\dot{m}_{cond}$ (kg/s)	$T_{evap,in}$ (°C)	$T_{cond,in}$ (°C)	N_{pp} (rpm)	N_{exp} (rpm)	$\dot{W}_{el,net}$ (kW)
1	35.13	0.220	0.260	85.15	13.89	600	900	0.301
2	34.94	0.220	0.259	84.99	13.85	600	1200	0.364
3	34.58	0.220	0.262	84.80	13.77	600	1500	0.419
4	48.89	0.220	0.262	84.53	13.72	800	1500	0.482
5	49.18	0.220	0.263	84.22	13.78	800	1800	0.531
6	73.72	0.330	0.553	86.80	12.88	1200	2700	0.781
7	74.26	0.330	0.551	86.29	12.88	1200	3000	0.798
8	74.41	0.330	0.556	85.36	13.02	1200	3250	0.809
9	49.99	0.150	0.445	84.68	13.67	830	1600	0.460
10	60.63	0.180	0.444	84.30	13.75	1000	2000	0.510
11	67.24	0.180	0.446	83.97	13.68	1100	2400	0.560
12	78.90	0.260	0.451	81.29	12.87	1250	3700	0.670
13	79.08	0.260	0.450	80.82	13.60	1250	4000	0.557
14	65.65	0.378	0.584	84.84	12.70	1060	3160	0.779
15	71.35	0.375	0.589	84.28	12.65	1140	3160	0.796
16	71.84	0.373	0.588	83.60	12.79	1140	3700	0.840
17	39.67	0.380	0.374	83.13	23.07	700	1500	0.411
18	40.05	0.380	0.367	82.92	22.81	700	2000	0.411
19	40.47	0.378	0.363	82.54	22.67	700	2500	0.382
20	40.36	0.376	0.365	82.11	22.63	700	2800	0.371
21	40.52	0.370	0.367	81.43	22.64	700	3100	0.307
22	46.45	0.360	0.429	83.99	27.75	800	1500	0.421
23	46.69	0.360	0.429	83.90	27.79	800	2000	0.443
24	47.04	0.360	0.426	83.68	27.61	800	2500	0.416
25	46.80	0.360	0.423	83.33	27.60	800	2800	0.379
26	46.90	0.360	0.425	82.89	27.60	800	3100	0.345
27	47.23	0.360	0.428	82.14	27.57	800	3500	0.255
28	52.49	0.360	0.418	84.37	27.23	900	1500	0.456
29	52.88	0.360	0.420	84.26	27.17	900	2000	0.498
30	53.25	0.360	0.421	83.95	27.07	900	2500	0.501
31	53.83	0.360	0.419	83.53	27.19	900	2800	0.463
32	53.53	0.360	0.415	82.99	27.11	900	3100	0.420
33	53.86	0.360	0.419	82.15	27.05	900	3500	0.334
34	58.07	0.360	0.425	83.84	27.76	1000	1500	0.431
35	58.47	0.360	0.420	83.76	27.61	1000	2000	0.512

36	58.88	0.360	0.418	83.64	27.70	1000	2500	0.578
37	59.61	0.360	0.417	83.41	27.62	1000	2800	0.517
38	59.96	0.360	0.417	83.00	27.54	1000	3100	0.492
39	59.99	0.360	0.417	82.56	27.45	1000	3500	0.392
40	60.14	0.360	0.419	81.93	27.52	1000	4000	0.330
41	65.54	0.360	0.420	83.96	27.28	1100	1500	0.425
42	66.00	0.360	0.423	83.95	27.23	1100	2000	0.522
43	66.30	0.360	0.417	83.87	27.11	1100	2500	0.562
44	66.67	0.360	0.417	83.75	26.98	1100	2800	0.582
45	66.64	0.360	0.422	83.62	27.14	1100	3100	0.584
46	67.61	0.360	0.421	83.25	27.06	1100	3500	0.545
47	67.16	0.360	0.424	82.93	27.25	1100	4000	0.425
48	66.74	0.360	0.424	82.56	27.42	1100	4500	0.292
49	73.50	0.360	0.422	85.58	27.09	1200	2000	0.541
50	74.03	0.360	0.421	85.38	27.24	1200	2500	0.691
51	73.55	0.360	0.422	85.17	27.25	1200	2800	0.608
52	74.09	0.360	0.419	84.79	27.28	1200	3100	0.620
53	73.85	0.360	0.418	84.35	27.34	1200	3500	0.579
54	73.67	0.360	0.426	84.04	27.23	1200	4000	0.503
55	74.02	0.360	0.423	83.37	27.26	1200	4500	0.390
56	66.87	0.429	0.422	83.31	27.74	1100	2000	0.515
57	66.64	0.430	0.423	83.30	27.71	1100	2500	0.663
58	67.51	0.430	0.426	83.18	27.49	1100	2800	0.586
59	67.06	0.430	0.423	82.82	27.29	1100	3100	0.586
60	66.46	0.430	0.418	85.56	27.25	1100	3500	0.555
61	66.95	0.430	0.424	85.40	27.35	1100	4000	0.578
62	67.26	0.430	0.423	85.36	27.55	1100	4500	0.435

Table 6: Measurement data (HP)

Test	$\dot{m}_{wf}$ (g/s)	$\dot{m}_{evap}$ (kg/s)	$\dot{m}_{cond}$ (kg/s)	$T_{evap,in}$ (°C)	$T_{cond,in}$ (°C)	N_{cmp} (rpm)	COP (-)
1	7.10	0.491	0.200	16.86	22.05	1300	7.294
2	8.34	0.489	0.200	17.02	22.79	1500	7.582
3	11.36	0.486	0.200	16.57	22.81	1800	8.390
4	11.69	0.490	0.200	16.30	23.68	2100	7.352
5	14.09	0.496	0.200	16.19	23.72	2500	7.193
6	17.53	0.480	0.200	16.61	24.43	2900	7.349
7	19.35	0.491	0.199	16.59	24.39	3300	6.509
8	6.80	0.140	0.200	13.87	22.96	1500	6.185
9	10.38	0.140	0.200	13.80	22.97	2000	7.343

10	9.73	0.204	0.230	26.73	35.01	1300	7.399
11	13.84	0.203	0.230	26.58	34.98	1700	8.086
12	16.90	0.202	0.230	26.58	35.02	2000	8.387
13	13.42	0.244	0.299	23.96	37.56	1800	6.670
14	17.18	0.245	0.300	23.95	37.57	2200	6.503
15	19.13	0.244	0.300	23.98	37.65	2500	5.855
16	22.86	0.292	0.299	25.83	36.37	2800	5.910
17	22.92	0.274	0.299	25.05	36.31	3000	5.441
18	27.37	0.347	0.200	22.65	40.92	3500	5.820
19	30.70	0.354	0.200	22.56	40.93	3900	5.845
20	15.73	0.225	0.220	25.71	46.94	2000	5.642
21	18.65	0.228	0.220	25.66	46.85	2300	5.633
22	19.70	0.249	0.269	30.33	61.47	2200	4.621
23	23.87	0.248	0.270	30.27	61.14	2500	4.674
24	27.60	0.247	0.270	30.20	60.83	2800	4.707
25	34.76	0.246	0.265	30.23	60.43	3200	4.832
26	35.80	0.269	0.270	30.96	57.32	3500	5.154
27	38.47	0.269	0.270	31.16	57.14	3800	5.136
28	40.87	0.269	0.270	31.06	56.91	4000	5.118
29	15.84	0.318	0.300	35.39	49.97	1500	6.666
30	23.27	0.317	0.296	35.65	49.87	2000	6.850
31	30.97	0.269	0.299	36.22	54.24	2500	6.348
32	37.15	0.269	0.300	36.21	54.04	3000	6.289
33	42.69	0.265	0.300	36.47	53.90	3400	6.282
34	46.63	0.271	0.300	36.49	53.94	3800	6.166
35	24.72	0.272	0.300	46.50	55.79	1500	8.264
36	34.69	0.277	0.300	46.50	55.54	2000	8.278
37	42.90	0.276	0.300	46.65	55.44	2500	8.076
38	51.52	0.276	0.299	46.70	55.30	3000	7.922
39	59.10	0.271	0.300	47.28	55.43	3500	7.848
40	63.47	0.271	0.300	47.61	55.25	4000	7.532
41	66.82	0.271	0.300	47.40	55.12	4200	7.511
42	60.40	0.299	0.279	74.51	74.53	1600	11.307
43	70.89	0.300	0.280	74.10	73.94	2000	10.309
44	75.27	0.302	0.279	74.47	73.48	2250	10.030
45	32.36	0.297	0.350	69.96	68.95	1000	13.487
46	29.00	0.402	0.259	69.03	70.42	900	12.591
47	42.14	0.402	0.259	68.59	70.18	1200	12.288
48	52.79	0.406	0.260	68.41	69.84	1500	11.996

49	73.44	0.406	0.260	68.50	68.99	2200	10.811
50	76.44	0.390	0.269	66.50	65.05	2500	11.444
51	84.25	0.386	0.270	66.11	64.28	2900	10.743
52	21.61	0.281	0.280	30.81	32.94	1900	13.761
53	17.30	0.277	0.279	30.91	32.41	1470	14.422
54	21.50	0.278	0.280	30.80	32.49	1900	13.569
55	26.18	0.277	0.280	30.76	32.60	2200	13.802
56	28.98	0.277	0.280	30.67	32.57	2500	13.610
57	35.01	0.280	0.280	30.60	32.50	2900	13.501
58	38.29	0.280	0.280	30.74	32.54	3300	12.915
59	40.10	0.280	0.280	30.68	33.79	3700	11.520
60	41.89	0.279	0.280	30.72	33.83	4100	10.978

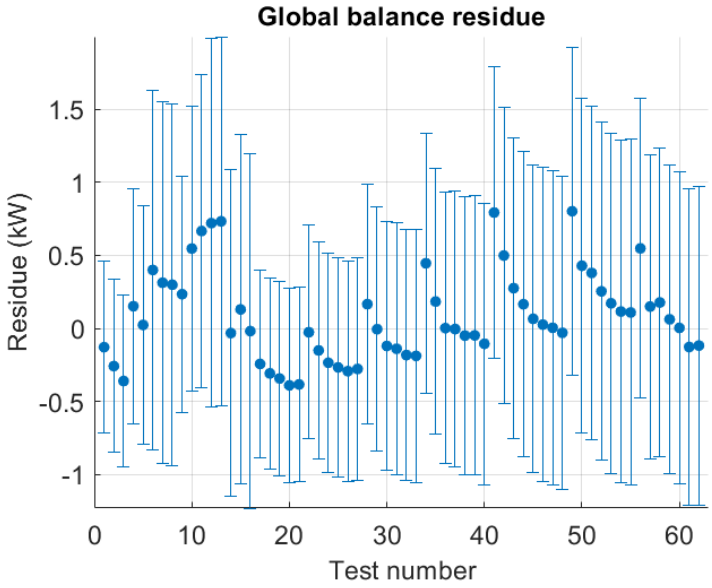

Figure 6: Global residual (ORC)

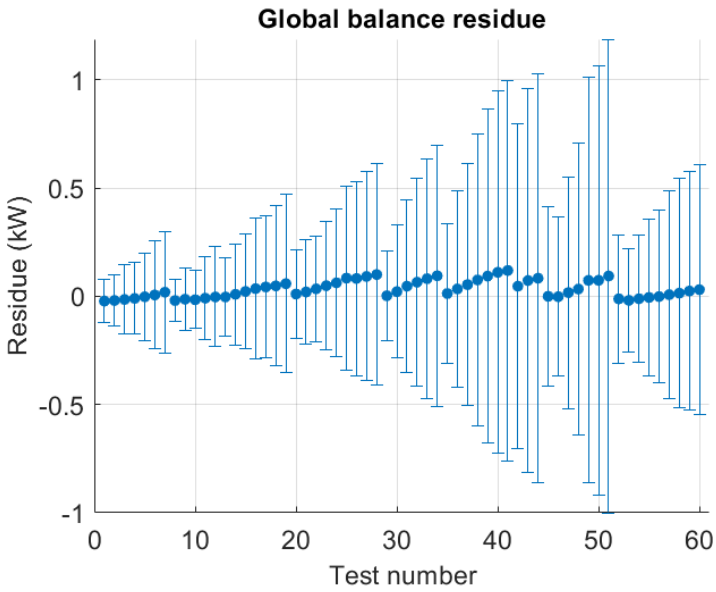

Figure 7: Global residual (HP)

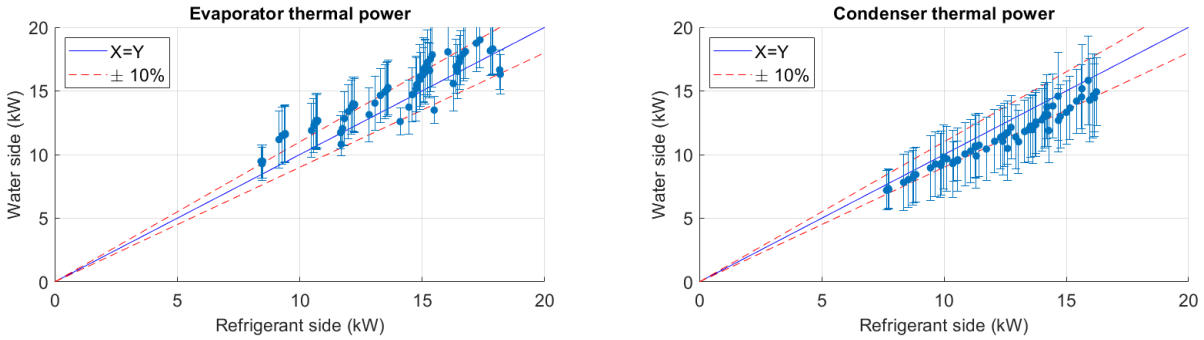

Figure 8: Heat exchangers energy balance (ORC)

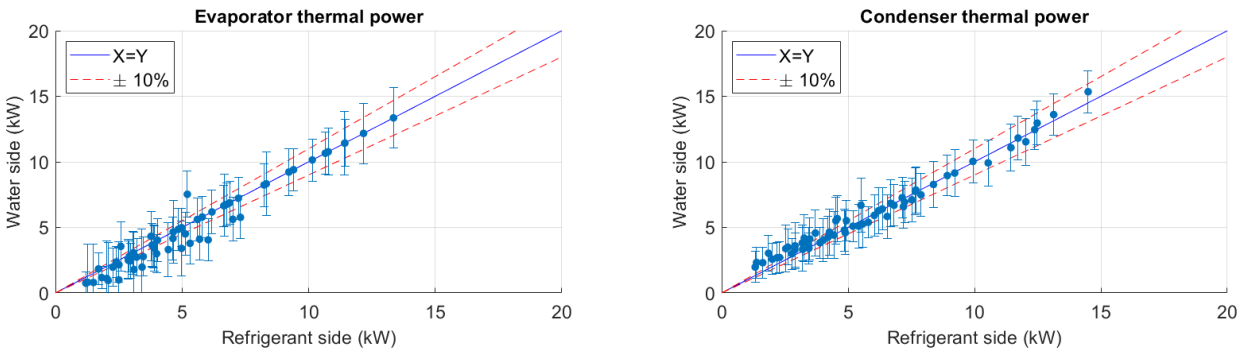

Figure 9: Heat exchangers energy balance (HP)

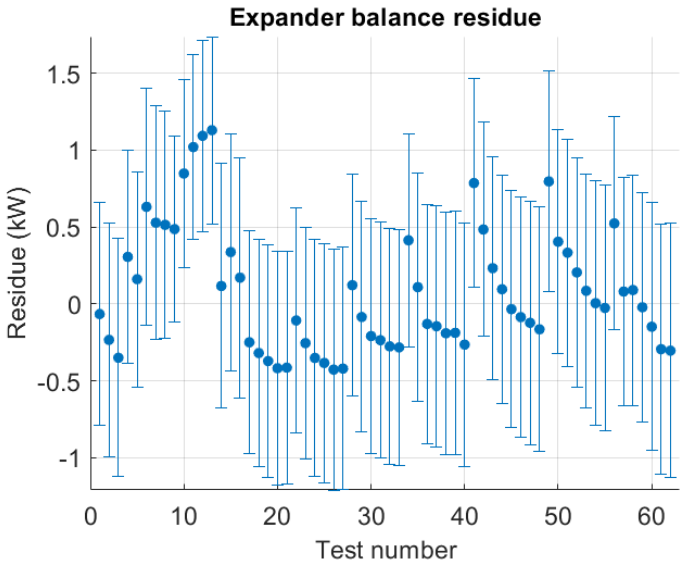

Figure 10: Expander energy balance (ORC)

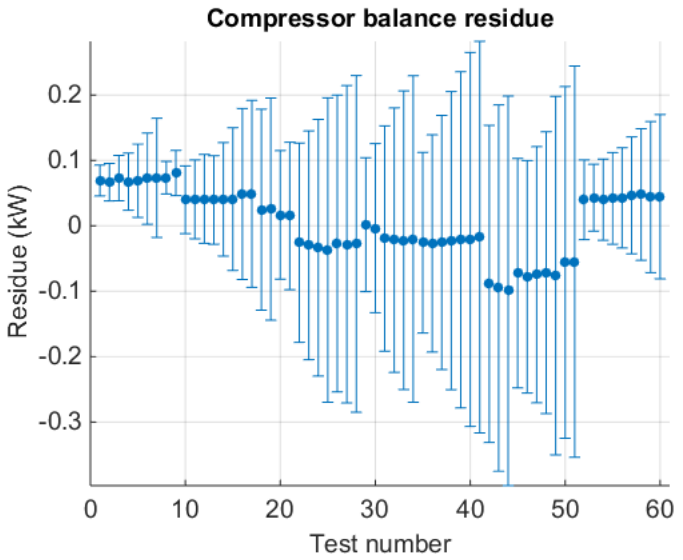

Figure 11: Compressor energy balance (HP)